Oceanic transport of subpolar climate signals to mid-depth subtropical waters

Ruth G. Curry, Michael S. McCartney & Terrence M. Joyce

Woods Hole Oceanographic Institution, Woods Hole, Massachusetts 02543, USA

The spatial distributions of certain sea-surface properties, such as temperature, fluctuate on timescales from months to decades and in synchrony with the main regional atmospheric patterns comprising the global climate system[1]. Although it has long been assumed that the ocean is submissive to the dictates of the atmosphere, recent studies raise the possibility of an assertive, not merely passive, oceanic role in which water-mass circulation controls the timescales of climate fluctuations[2–6]. Previously held notions of the immutability of the physical and chemical characteristics of deep water masses are changing as longer time series of ocean measurements indicate that the signatures of varying sea-surface conditions are translated to deep waters[4,7]. Here we use such time-series measurements to track signals 'imprinted' at the sea surface in the North Atlantic Ocean's subpolar Labrador Basin into the deep water of the subtropical basins near Bermuda, and infer an approximately 6-year transit time. We establish a geographic and temporal context for a portion of the long-term warming trend reported for mid-depth subtropical waters over the past 40 or so years[8,9], and we predict that waters at these depths will continue to cool well into the next decade.

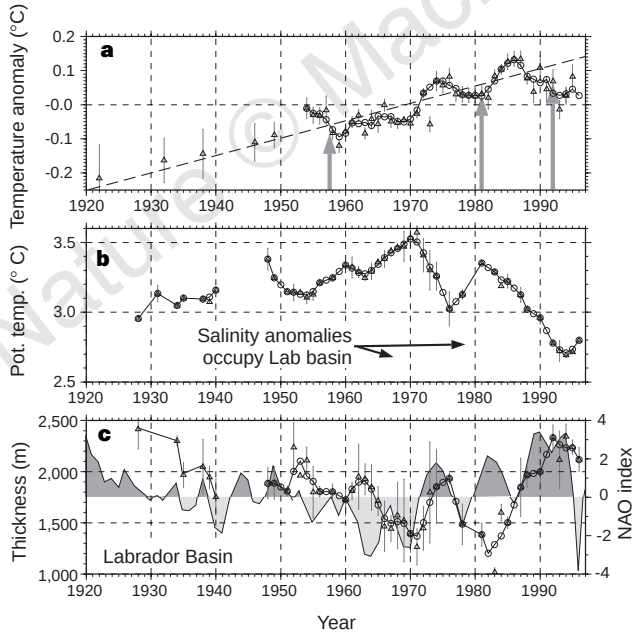

Figure 1 Evolution of subtropical and subpolar water masses through time. **a**, Time series of subtropical temperature anomaly in 1,500–2,500-m layer near Bermuda[9]. Triangles are annual mean, vertical bars are s.d. Circles and curve depict 3-year smoothed values. The broken line is a warming trend inferred from data[9]. Arrows indicate years from which section data were compared to deduce a similar warming trend[8,10]. **b**, Potential temperature of LSW core (at 1,500 m) in its subpolar formation area. Means and standard deviation are as in **a**. Cross-hatched years delimit periods during which fresh water capped the Labrador basin. Data source is HydroBase[20]. **c**, Thickness of LSW density layer ($\sigma_{1,500}$ = 34.62–34.72) in its formation area. The NAO index of Hurrell[14] is overplotted with high index years shaded dark and low index years shaded lightly.

Warming of the subtropical mid-depths has been deduced by a variety of techniques including the comparison of zonal[8,10] and meridional[9] temperature sections from different years, temperature-mapped on depth surfaces[11] from different time windows, and from analyses of the temperature–depth time series maintained near Bermuda[9,12]. A trend analysis (broken line in Fig. 1a) of this time series, reproduced in Fig. 1a, implies a warming of 0.5 °C per century over the 70-year record[9]. The densely sampled years after 1954 show decadal oscillations superimposed on the long-term trend[9,12], and, by linking the time series analysis with the changes observed in temperature sections from different years[8–10], a 1,000-km scale variability at 10-year timescales is inferred for the western basin[8,9].

Over the same period, subpolar mid-depth conditions in the Labrador basin show a long-term warming trend from the 1920s to 1971 that ends abruptly in 1972 and is followed by a cooling trend that persists to the present[13]. A time series of temperature of the Labrador Sea Water (LSW) core measured in its source region (Fig. 1b) illustrates these trends. Formed by deep wintertime convection in the Labrador basin, the LSW is characteristically cold, fresh and very thick compared with other North Atlantic water masses of similar density. The time history of LSW thickness—defined here by the vertical distance between two density surfaces—approximately mirrors the temperature trends (Fig. 1c): the long period of warming before 1972 corresponds to a thinning of the layer, whereas the cooling years of the 1970s and after 1983 are accompanied by layer thickening. The thickness of the LSW layer is directly related to the intensity of wintertime convection: strong convection produces a thick layer, and weak convection results in a relatively thin layer.

The depth of Labrador basin convection is principally determined by the strength of the westerly winds and the occasional passage of freshwater surface anomalies[4,7,13]. Also possibly involved are anomalies of SST and heat content carried from the subtropics into the subpolar gyre[5,19]. An increase in wind strength removes more heat from the surface waters and deepens the extent of convection. This also results in a cooler overall LSW, because the increased heat loss at the sea surface is distributed downward as the water column overturns. The North Atlantic Oscillation (NAO) index[14], which represents the relative strength of the westerlies, is overplotted on the LSW thickness axis (Fig. 1c) and shows trends similar to the LSW properties: declining NAO index (weakening winds), thinning and warming LSW from 1950s to 1970, a pulse of strong westerly winds (high index), LSW thickening and cooling in the early 1970s followed by weak westerlies (low index) and thin conditions in the late 1970s, then extremely strong westerlies, thick and cold LSW in the 1990s. There is a suggestion of perhaps a 2–4-year time lag between the atmospheric NAO and LSW thickness indices, which is indicative of the ocean's slower response time. The wind strength briefly loses its influence on LSW conditions during occasional salinity events: the thin LSW layers of 1968–72 and the early 1980s

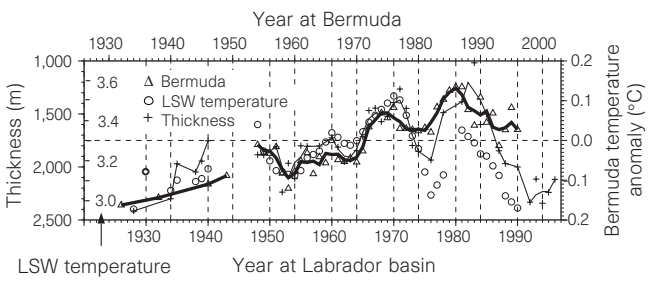

Figure 2 Bermuda temperature anomaly from Fig. 1a lagged by 6 years (triangles, thick curve) with LSW source thickness (thin curve and + symbols; axis has been inverted compared with Fig. 1c) and LSW core temperature (circles). After 1990, LSW temperatures are colder than 2.9 °C and are not visible in this plot.

correspond to buildups of extremely low surface salinities, which completely inhibited convective overturning[4,7,13]. The first of these two events, referred to as the 'great salinity anomaly'[15], occupied the Labrador basin during a time of low NAO index when weak westerlies would have resulted in weak convection anyway. Note that the warming and thinning trend spans two decades, mirroring the general decline of the NAO index of the 1950s and 1960s, whereas the low-salinity event occurs in 1968–72, only at the very end of the trend. However, the second event, the 'lesser great salinity anomaly'[16], shut down convection in the early 1980s causing the LSW to become thinner despite strong westerlies associated with a relatively high NAO index. Both events ended with a strong increase in convection and a downward mixing of the chilled freshwater cap, which markedly lowered the LSW core temperature (Fig. 1b) and salinity[12].

The subpolar LSW enters the subtropics via two principal pathways: the deep western boundary current (DWBC) advects LSW southward to the tropics, whereas the Gulf Stream and North Atlantic Current transport it from the western boundary out into the basin interior[17]. The LSW in those flows is strongly stirred and mixed by the action of recirculations and eddies along these pathways. The subtropical basin-scale deep-water properties thus represent an advective–diffusive blending of the cold, fresh, thick LSW with other influences such as the warm, salty, thin Mediterranean Outflow Water (MOW); the resulting water mass, Upper North Atlantic Deep Water (UNADW), exhibits a temperature history that we can now relate to variations in the LSW source as follows. Over the past century, the volume of LSW flowing out of the subpolar gyre has increased/decreased as this water mass has thickened/thinned. A decrease in LSW entering the subtropics causes a relative ascendancy of the MOW characteristics and results in a warmer, saltier and thinner UNADW layer. Conversely, an increased volume of LSW results in fresher, cooler, thicker UNADW. The time required to advect and mix the LSW into the subtropics introduces a time delay to the link between these signals.

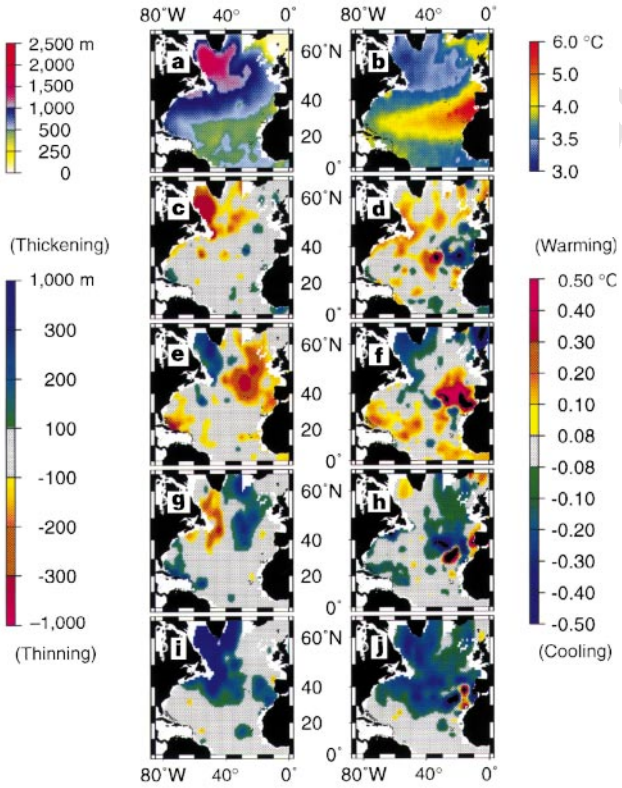

Figure 3 Anomalies of thickness and temperature propagate away from their subpolar source. **a**, Mean thickness of the density layer corresponding to Labrador Sea Water ($\sigma_{1,500} = 34.62$–34.72) over the entire North Atlantic. Data source is HydroBase[20]. **b**, Potential temperature (climatological mean) on a density surface in the middle of the LSW layer ($\sigma_{1,500} = 34.67$). **c**, Change in thickness of LSW layer mapped in **a** between two time periods: 1966–72 compared with 1957–65. Blue–green colours correspond to layer thickening in the later time compared with the earlier; yellow–red colours indicate layer thinning. **d**, Change in temperature on the density surface mapped in **b** for the time periods compared in **c**. Blue–green colours correspond to cooling in the later time compared with the earlier; yellow–red colours indicate warming. **e**, **f**, Thickness and temperature change: 1973–79 compared with 1966–72. **g**, **h**, Thickness and temperature change: 1980–86 compared with 1973–79. **i**, **j**, Thickness and temperature change: 1987–94 compared with 1980–86.

When a time lag is applied to the Bermuda temperature anomaly signal (from Fig. 1a), the subpolar and subtropical records are strikingly similar both over the long term (70 years) and at decadal timescales (Fig. 2). The coldest, but very sparse, Bermuda data before 1950 correspond to thick and cold LSW conditions. From 1922 to 1987 Bermuda exhibits a general warming, whereas the LSW exhibits an overall thinning from 1928 to 1983. The LSW began to thicken and cool around 1982, reaching extreme values in the 1990s; Bermuda temperatures began to cool in 1988. The subpolar LSW pulsed cooler and thicker for 4 years in the 1970s, which is echoed by a limited cooling at Bermuda from 1977 to 1982, but did not reverse the subtropical warming trend. Negative correlation between the subtropical temperature and subpolar thickness signals is strongest ($r < -0.6$) at lags of 5–7 years and implies that when subpolar convection is strong—and the LSW layer is thick—the subtropics follow about 6 years later with cooler UNADW temperatures. Conversely, weak convection and a thin LSW layer are followed by warmer UNADW. The lag is not precise because the basin-scale advective–diffusive mixing is not an exact process, and because earlier measurements in both time series were less abundant and also made with cruder technology.

To place this relationship into a geographic context, Fig. 3a maps the thickness of the LSW density layer ($\sigma_{1,500} = 34.62$–34.72) and Fig. 3b maps the temperature on a density surface ($\sigma_{1,500} = 34.7$) in the middle of that layer. We use density as opposed to depth surfaces because adjacent water masses mix predominantly along these isopycnal surfaces, which vary greatly in depth from the subpolar (500 m) to subtropical gyre (1,800 m). In Fig. 3a the red colours indicate thicknesses exceeding 2,000 m in the LSW source region. The green tongue (thickness < 500 m) stretching westwards across the subtropics delineates where MOW influences are strong; deep blue colours represent waters whose properties (thickness, temperature, salinity, and so on) are intermediate between the LSW and MOW sources. In Fig. 3b the LSW is identified by coldest temperatures (blue colours), the MOW shows as the red–yellow tongue, and the product of their mixing is green.

The remaining panels of Fig. 3 demonstrate the time-lagged impact of LSW temperature and thickness anomalies on the subtropics. Here we subdivided the post-1956 data into five periods, each spanning 7–8 years, and mapped the thickness and temperature differences in one time frame compared with its preceding time frame. The alternating yellow–red (thinning, warming) and blue–green (thickening, cooling) patches in the Labrador basin depict the waning and waxing through time of LSW in its source region. These patterns also show large areas where thickness changes are correlated with temperature changes—that is, where the layer thins temperatures are warming, and where the layer thickens temperatures are cooling—and depict where LSW exerts a strong influence. In the eastern basin the main impact of the LSW thickness anomalies are restricted to the area north of 30° N, whereas in the western basin they are intensified towards the west but extend down to the tropics. These patterns also show consecutive instances where temperature and thickness anomalies of one sign first appear in the Labrador basin, are quickly advected southwards and eastwards by

the DWBC and North Atlantic Current (e.g. in Fig. 3c and d, where anomalies have same colour as in the Labrador basin) and then, one time frame later, anomalies of the same sign appear in both the western and eastern subtropical basins. This is consistent with the time lag implied by the Bermuda temperature/Labrador basin thickness correlation. The eastern subpolar gyre shows a similar delay, which is consistent with inferred influence times since the 1980s[14,18].

The time-delayed subtropical temperature patterns seem to represent the slow adjustment of the subtropical deep water's advective–diffusive balance to the waxing and waning LSW. As the LSW source thickens, its role in that balance strengthens and this is manifested as an eastwards and southwards erosion of the MOW influence on the subtropical deep water and thus cooler and fresher UNADW. The time required for the advective elements to circulate and mix the LSW into the subtropical basins results in a delayed appearance of the response. When the LSW is thinner than normal, the MOW is able to exert more influence on the advective–diffusive balance, and this appears as a westwards and northwards extension of its warm, salty and thin characteristics.

Understanding the nature of the subtropical temperature response and knowing that subpolar convection has been extreme from 1988 to 1995 prompts us to speculate that the subtropical mid-depths will continue to cool throughout the 1990s and the early 2000s. The cold, fresh and thick signal now invading the subtropics is quite pronounced in the bottom panels of Fig. 3 and will undoubtedly have profound effects on the UNADW properties. The colder, fresher UNADW arrived at Bermuda in August 1996. And its arrival in the DWBC at 26° N was noted by increased chlorofluorocarbon concentrations in 1996 by Miami researchers[19] who have been monitoring this region for about a decade. If the NAO index were to remain persistently high and subpolar convection strong, then the 40-year warming of the subtropical mid-depths would reverse to a substantial cooling. A switch from the high NAO of the 1980s and early 1990s to a persistent low index with weak subpolar convection, however, would again reduce the amount of LSW entering the subtropics and this impending cooling could appear as just another decadal oscillation in the long-term record. Such a switch might be in progress, for the NAO index has been low for two consecutive winters: 1995/96 and 1996/97. □

Received 17 March; accepted 14 October 1997.

1. Deser, C. & Blackmon, M. Surface climate variations over the North Atlantic Ocean during winter: 1900–1989. *J. Clim.* **6,** 1743–1753 (1993).
2. Kushnir, Y. & Held, I. M. Equilibrium atmospheric response to North Atlantic SST anomalies. *J. Clim.* **9,** 1208–1220 (1996).
3. Griffies, S. M. & Bryan, K. A predictability study of simulated North Atlantic multidecadal variability. *Clim. Dyn.* **13**(7/8), 459–487 (1997).
4. Dickson, B. From the Labrador Sea to global change. *Nature* **386,** 649–650 (1997).
5. Sutton, R. T. & Allen, M. R. Decadal predictability of North Atlantic Sea surface temperature and climate. *Nature* **388,** 563–565 (1997).
6. McCartney, M. S. Is the ocean at the helm? *Nature* **388,** 521–522 (1997).
7. Dickson, R., Lazier, J., Meincke, J., Rhines, P. & Swift, J. Long-term coordinated changes in the convective activity of the North Atlantic. *Prog. Oceanogr.* **38,** 241–295 (1996).
8. Bryden, H. L. *et al.* Decadal changes in water mass characteristics at 24° N in the subtropical North Atlantic Ocean. *J. Clim.* **9,** 3162–3186 (1996).
9. Joyce, T. M. & Robbins, P. The long-term hydrographic record at Bermuda. *J. Clim.* **9,** 3121–3131 (1996).
10. Roemmich, D. & Wunsch, C. Apparent changes in the climatic state of the deep North Atlantic Ocean. *Nature* **307,** 447–450 (1984).
11. Levitus, S. Interpentadal variability of temperature and salinity at intermediate depths of the North Atlantic Ocean, 1970–1974 versus 1955–1959. *J. Geophys. Res.* **94,** 6091–6131 (1989).
12. Houghton, R. W. Subsurface quasi-decadal fluctuations in the North Atlantic. *J. Clim.* **9,** 1363–1373 (1996).
13. Lazier, J. R. in *Natural Climate Variability on Decade-to-Century Time Scales of Natural Climate Variability* (ed. Martinson, D. G. *et al.*) 295–302 (National Academy Press, Washington, DC, 1995).
14. Hurrell, J. W. Decadal trends in the North Atlantic Oscillation: regional temperatures and precipitation. *Science* **269,** 676–679 (1995).
15. Dickson, R., Meincke, J., Malmberg, S.-A. & Lee, A. The "Great Salinity Anomaly" in the northern North Atlantic 1968–1982. *Prog. Oceanogr.* **20,** 103–151 (1988).
16. Belkin, I. M., Levitus, S. & Antonov, J. "Great Salinity Anomalies" in the North Atlantic. *Prog. Oceanogr.* (in the press).
17. Talley, L. D. & McCartney, M. S. Distribution and circulation of Labrador Sea Water. *J. Phys. Oceanogr.* **12,** 1189–1205 (1982).
18. Sy, A. *et al.* Surprisingly rapid spreading of newly formed intermediate waters across the North Atlantic Ocean. *Nature* **386,** 675–679 (1997).
19. Molinari, R. *et al.* Fast-track for recently formed Labrador Sea Water: the Deep Western Boundary Current of the North Atlantic Ocean. *Deep-Sea Res.* (submitted).
20. Curry, R. HydroBase: a database and tools for climatologic analysis. (Tech. Rep. WHOI-96-01, Woods Hole Oceanographic Inst, 1996).

Acknowledgements. This work was supported by the Atlantic Climate Change Program of NOAA's Climate and Global Change Program and by the National Science Foundaiton.

Correspondence and requests for materials should be addressed to R.G.C. (e-mail: rcurry@whoi.edu). Data available from flotsam.whoi.edu (128.128.28.187). cd pub/nature/curry_etal.

The generation of plankton patchiness by turbulent stirring

Edward R. Abraham

National Institute of Water and Atmospheric Research, P.O. Box 14-901, Kilbirnie, Wellington, New Zealand

Diffusive processes are often used to represent the formation of spatial patterns in biological systems[1]. Here I show how patchiness may be generated in planktonic ecosystems through non-diffusive advection. Plankton distributions in oceanic surface waters can be characterized by the spectra of concentrations obtained along ship transects. Such spectra are inevitably found to have a power-law form over horizontal scales ranging from 1 to 100 km (ref. 2). Phytoplankton have distributions similar to those of physical quantities such as sea surface temperature, with much less variability at shorter length scales. In contrast, zooplankton density may be almost as variable at short scales as long ones[3]. Distributions of this form are generated in a model of the turbulent stirring of coupled phytoplankton and zooplankton populations. The characteristic spatial patterns of the phytoplankton and zooplankton are a consequence of the timescales of their response to changes in their environment caused by turbulent advection.

The accuracy with which the ensemble-averaged dispersal of passive tracers in turbulent ocean flows may be described by eddy diffusion[4] has encouraged the use of diffusion-based models to study the generation of patchiness in planktonic ecosystems[5–8]. Diffusion causes variability to be transferred from small to large length scales, and so it is widely believed that "in order to be able to form a more finely grained pattern the zooplankton must have some

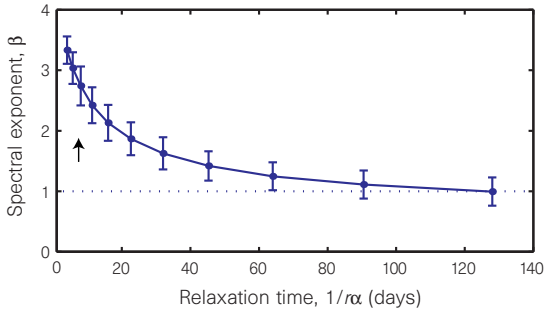

Figure 1 The phytoplankton carrying capacity relaxes towards a smoothly varying background value at a rate α, following equation 1. The power spectrum of a transect, $C(y)$, has the form $\tilde{C}(k) \propto k^{-\beta}$, where the spectral exponent, β, depends on the relaxation rate. Values are mean ± standard deviation of the exponents at the end of a high-resolution model run, calculated from 256 evenly spaced transects by linear regression of $\log(\tilde{C}(k))$ on $\log(k)$. With a relaxation time of $1/r\alpha = 8$ d the spectrum has an exponent $\beta_C = 2.74 \pm 0.32$ (arrow); this value of α is used in the text. The broken line marks the spectral exponent expected for a passive non-reacting tracer.